V. Bicego and C. Rinaldi**

Fractographic Study of Toughness Variability in the Transition Region

REFERENCE Bicego, V., and Rinaldi, C., **Fractographic study of toughness variability in the transition region**, *Defect Assessment in Components – Fundamentals and Applications*, ESIS/EGF9 (Edited by J. G. Blauel and K.-H. Schwalbe) 1991, Mechanical Engineering Publications, London, pp. 459–475.

ABSTRACT In the frame of an extensive fracture toughness characterisation of a SA533B steel, results of 23 tests performed in the brittle–ductile transition regime were analysed and the fracture surfaces of the specimens carefully examined through scanning electron microscopy. The values of the *J*-integral at the onset of the final brittle fractures were correlated to variations of three fractographic quantities, namely the stretch zone width, the amount of stable crack extension, and the distance of the cleavage origin from the tip of the ductile crack. To describe the relationship found a simple formula was proposed, in line with considerations of fracture phenomena in the literature, which successfully explained the large variations of the toughness data within 5 percent average error.

Notation

A	Plastic work, area under the load–displacement curve
a	Crack length
ao	Initial crack length
b	Specimen ligament ($W-a$)
B	Specimen thickness
J	J-integral
J_{ic}	Critical J
J_{inst}	Value of J at specimen failure by cleavage
$J_{inst,\,c}$	Calculated value of J_{inst}
K	Stress intensity factor
K_{ic}	Critical K
SZW	Stretch zone width
X	Distance of cleavage origin from ductile crack front
W	Specimen width
ν	Poisson's ratio
σ_y	Yield stress
σ_{uts}	Tensile strength
Δa	Ductile crack extension (stable tearing)

Introduction

The final failure event of a material in the brittle–ductile temperature transition regime is cleavage instability, following a small amount of ductile crack extension. In this case valid toughness data (K_{ic}, J_{ic}) are not normally

* CISE SpA, Via Reggio Emilia 39, 20090 Segrate Milano-I, Italy.

obtained from laboratory tests, and alternative toughness parameters are often considered. In addition to the large scatter experienced by these data, one is also generally faced with the uncertain application of invalid toughness parameters to real structural situations: thickness dependence is a typical problem. In order to define the criteria for applicability of laboratory data to plant situations, to develop appropriate statistics for the relevant toughness parameters, and to define reliable lower bounds for safe engineering applications, a better understanding of the failure events in the transition region is essential.

It is generally recognised that the large scatter in toughness data resulting from laboratory tests in the transition region occurs in conjunction with different extents of stable crack growth, implying a high-energy ductile rupture mechanism **(1)–(3)**. As these amounts are finally determined by the onset of the final brittle instability, cleavage triggering is the leading event. This is generally considered a stochastic phenomenon, to be treated in statistical terms **(4)**. A wide discussion is going on concerning the most appropriate statistical distribution applicable **(5)–(7)**; typically these approaches require many tests at several defined temperatures **(8)**, and seem correctly applicable only to laboratory data when a single fracture mechanism is present **(3)**.

In the effort of contributing to explain the high amount of scatter and the size effect for toughness data in the transition region, fractographic investigations are also increasingly undertaken **(2)(3)(9)**. Following this approach, the present study, based on quantitative fractography, analyses the correlations between toughness data and fractographic parameters representative of the failure mechanisms leading to the final brittle rupture. The proposed equation gives a clear picture of the failure phenomenon in the transition region even on a basis of small numbers of tests, performed at various temperatures.

Material and experimental

In the frame of an ENEL/DSR (Italian Electricity Board/R and D Division) project focused on fracture behaviour of structural materials for plant components under elastic and elasto-plastic conditions, an extensive fracture toughness characterisation was carried out at CISE on a ASTM SA533B CL1 steel. The material for the tests was derived from three plates; chemical composition, main mechanical properties, and heat treatments are summarised in Table 1. Plain sided and 20 percent side grooved Compact Tension specimens of different sizes, 1–4 inches thick, were tested at various temperatures, −190°C to +288°C. A comprehensive report of results from the main characterisation is contained in **(10)**.

In this study the attention was restricted to 1TCT (1 inch thick compact tension) specimens failed by cleavage instability in the temperature transition region, −130 to −20°C. The analysis considered the values of J_{inst}, the J-integral at the instant of final failure of the specimen by cleavage instability.

Table 1 The SA533B steel plates

Chemical composition (wt%)

Plate	*C*	*Mn*	*P*	*S*	*Si*	*Ni*	*Mo*	*Cr*	*Cu*	*Al*	*V*
W	0.19	1.48	0.011	0.007	0.20	0.56	0.53	0.12	0.17	0.016	0.003
X	0.21	1.43	0.006	0.011	0.23	0.62	0.50	0.08	0.08	0.016	
V	0.20	1.40	0.007	0.006	0.23	0.65	0.51	0.15	0.04	0.027	0.01

Tensile and impact properties

Plate	*Thickness (mm)*	*Grain size ASTM N°*	σ_y *(MPa)*		σ_{uts} *(MPa)*		*FATT* (°C)*	
			−80°C	*25°C*	*−80°C*	*25°C*	*LT*	*TL*
W	140	8.5	498	446	678	598	−14	−6
X	136	9.5–10	513	450	690	598	0	
V	136	7.5	518	450	685	586	−41	−13

Heat treatments

Plate	*Austenitizing* (°C)	*Austenitizing* (h)	*Quenching*	*Tempering* (°C)	*Tempering* (h)	*Stress relieving* (°C)	*Stress relieving* (h)	*Stress relieving cool to*	*Stress relieving* (°C)
W	900	4	water	650	6	610	3	furn.	315
						+610	6	furn.	315
X	880	3.5	water	650	5	610	6	furn.	315
V	844–910	5.5	water	660	5.2	610	36	furn.	315
						+610	25	furn.	300

* FATT = Fracture appearance transition temperature

Whenever the amounts of subcritical crack extensions (Δa) were in excess of $\Delta a = 0.1\ b$ (b = specimen ligament, this being the condition for a valid J-field to exist in the specimens), the data were rejected. Values of J_{inst} were evaluated according to ASTM E813–87

$$J = Je + Jp \tag{1}$$

$$Je = \frac{K^2(1-\nu^2)}{E} \tag{2}$$

$$Jp = \frac{(2 + 0.522(W - ao))A}{B(W - ao)} \tag{3}$$

with W = specimen width, B = specimen thickness, ao = initial crack length, A = plastic work area under the load–displacement curve, and K = the stress intensity factor, a function of the applied load and of the specimen geometry, evaluated according to standard formulae in LEFM handbooks and also reported in ASTM E813–87.

The fracture surfaces of twenty-three 1TCT specimens, tested in the temperature range −130 to −20°C, were carefully examined by scanning electron microscopy in order to locate the cleavage triggering point. Although several apparent cleavage origins could be found in some cases on the same specimen,

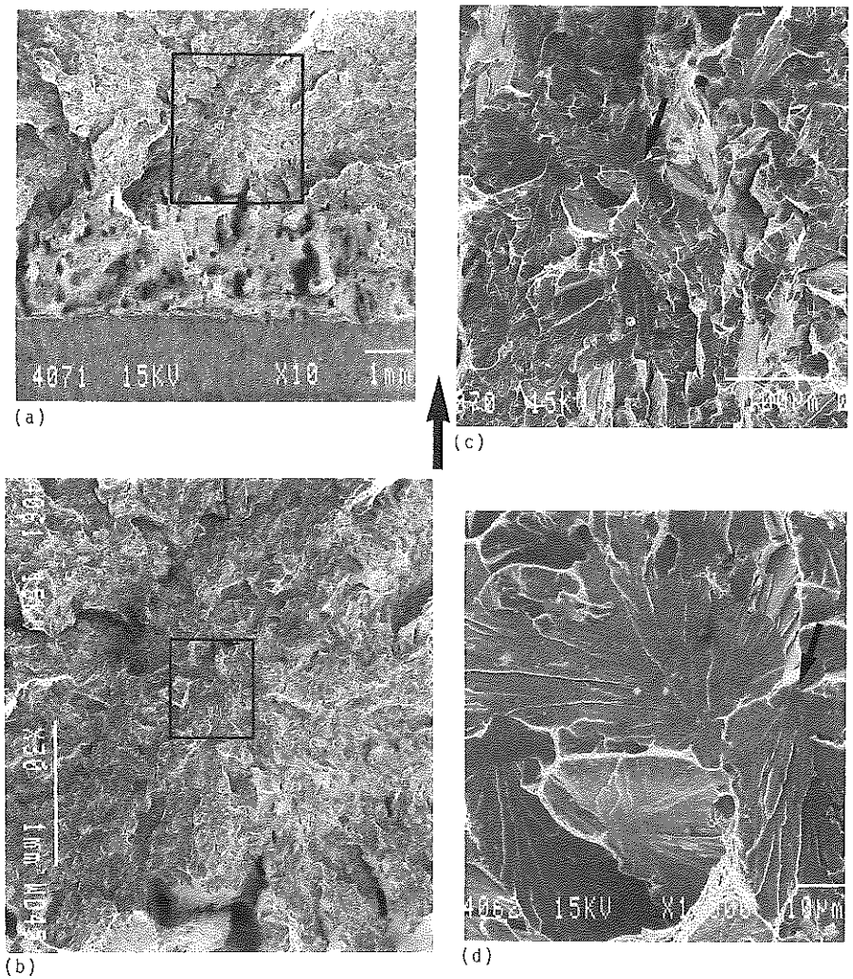

Fig 1 Sequence of fracture micrographs at increasing magnifications, for main cleavage origin identification

only the main point at the centre of the tear ridges visible at very low magnification ($\times 10$), was considered. The analysis of this region was performed at progressively increasing magnifications, following the river markers on cleavage facets, Figs 1 and 2. Identification of the cleavage origins was possible even at the highest temperatures considered, where the appearance of groups of facets with spiral arrangements led to some difficulty in the exact location of the triggering point, Fig. 1(d); in all cases a useful tool was to find out and follow the groups of cleavage facets back-oriented towards the ductile crack front.

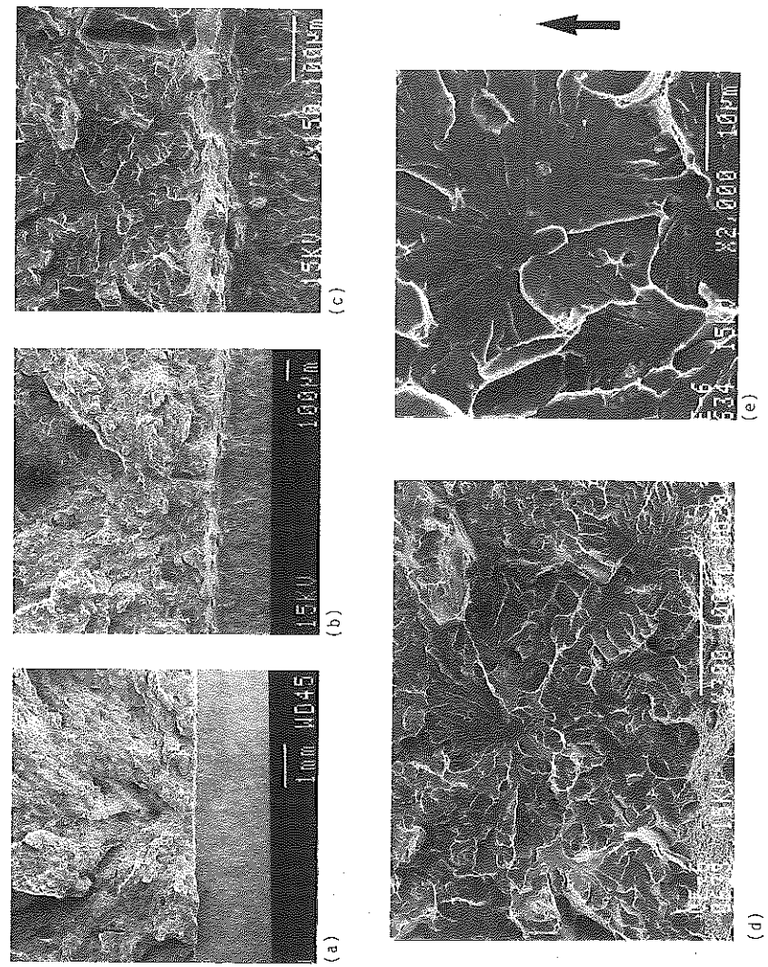

Fig 2 Example of main cleavage origin identification; note the absence of any microstructural feature at the triggering point, typical of 70 percent of the specimens observed

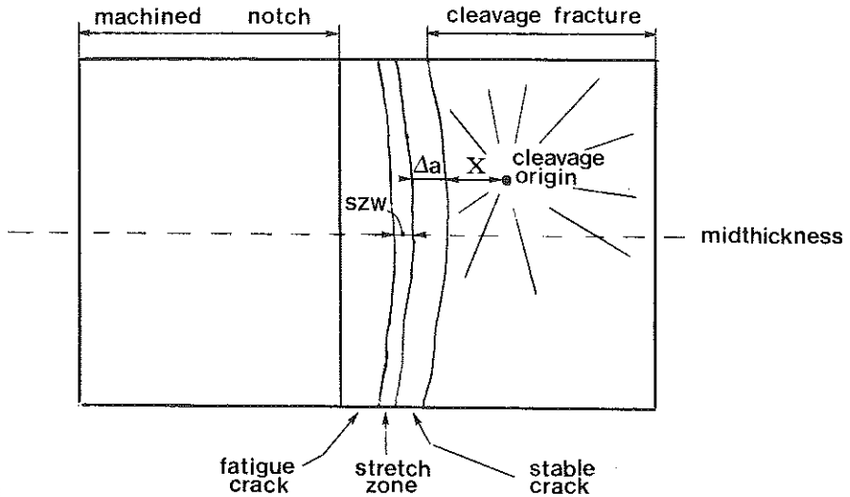

Fig 3 A view of the definitions adopted for SZW; *a*, and *X*

Three parameters representative of different stages of failure were defined and measured (Fig. 3).

- SZW = the stretch zone width, inside a region around the mid-thickness of the specimen;
- Δa = the ductile crack extension (i.e., considering only the tearing portion and excluding the stretch zone), measured at the position corresponding to the cleavage triggering point;
- X = the distance of the origin of cleavage from either the stable ductile crack or the blunted fatigue crack, in the absence of ductile tearing.

A particular measuring procedure was established to assure optimum reproducibility of data: SZW and Δa were measured at five equi-spaced positions within a 2 mm wide region; the region was centred at the specimen mid-thickness when measuring SZW, and at the cleavage origin when measuring Δa.

Results

The results obtained here represent an extension to the bainitic A533B steel of analyses already performed by other authors, who successfully demonstrated for forged A508 **(2)** and NiCrMoV rotor **(3)** steels the possibility to locate the cleavage triggering points in transition temperature regime of toughness.

Interestingly, at the identified cleavage origins no evidence of microstructural features acting as a possible source of local material weakening was found in 70 percent of the specimens analysed, Fig. 2(e). Among the other specimens, one half revealed small voids, possibly carbide sites, Fig. 4; the remaining

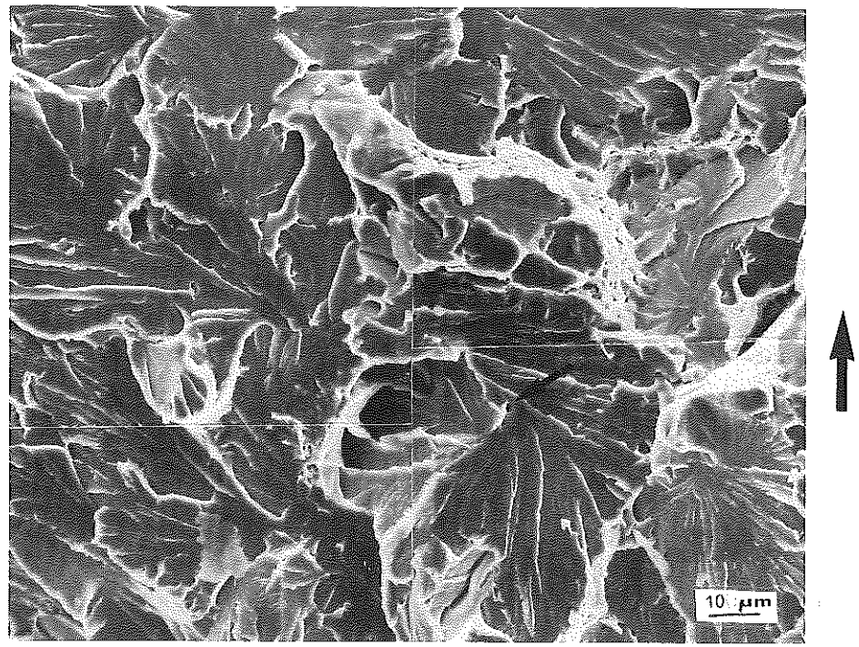

Fig 4 Example of small voids, possibly carbide sites, found at the cleavage triggering point of only 15 percent of the specimens

specimens showed local intergranular de-cohesions, mainly at low temperature, Fig. 5. Inclusions families had an indirect role, altering stress–strain fields ahead of the ductile crack tips through cavity formation around them; this happened particularly at high temperature.

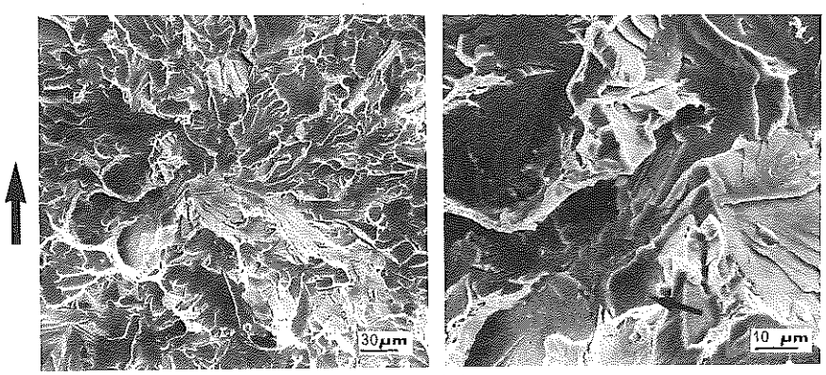

Fig 5 Example of local intergranular failure at the cleavage triggering point

Table 2 Fracture toughness data and results from the fractographic analysis

Temperature (°C)	J_{inst} (*KN/m*)	*SZW* (*mm*)	Δa (*mm*)	X (*mm*)
−130	20.6	0.010	0	0.045
−100	107.6	0.043	0.035	0.175
−100	109.0	0.042	0.030	0.180
−80	118.7	0.052	0.025	0.280
−60	30.6	0.015	0	0.023
−60	37.5	0.021	0	0.082
−60	38.3	0.014	0	0.283
−60	100.9	0.037	0.031	0.211
−60	126.7	0.052	0.031	0.200
−60	130.6	0.053	0.043	0.123
−60	135.4	0.051	0.025	0.660
−60	157.2	0.067	0.062	0.280
−60	174.5	0.067	0.065	0.500
−60	206.9	0.084	0.104	0.423
−60	211.0	0.082	0.140	0.540
−40	195.0	0.045	0.242	0.876
−40	201.3	0.083	0.090	0.337
−40	207.5	0.083	0.094	0.251
−40	213.0	0.074	0.172	0.588
−40	234.5	0.077	0.261	0.700
−40	250.1	0.077	0.239	0.312
−20	331.6	0.108	0.251	0.558
−20	677.7	0.094	2.429	1.450

Results from the fracture toughness tests and from the fractographic measurements over the 23 specimens considered in this investigation are reported in Table 2. As expected in the transition region, a relevant scatter is present, as clearly shown by the group of tests carried out at −60°C. All fractographic data show a tendency to increase as long as temperature and J_{inst} values increase.

Analysis

An analysis over the variability of data of J_{inst} was performed, the objectives being:

- to verify if the highly scattered values of J_{inst} could be related to the variations of fractographic parameters;
- to provide a picture of the failure phenomenon in the transition region in terms of a simple equation.

In general the value of the *J*-integral at the onset of cleavage fracture depends on a number of factors: the temperature, the specimen size (perhaps even the shape and the loading mode; here only tests on 1TCT specimens are considered), and features of the microstructure. Despite the complexity in the mechanisms involved, the typical aspect of a specimen fractured in the transition region reflects the three main stages of failure: initial yielding and crack

tip blunting, ductile crack extension, and final brittle fracture by cleavage instability, originated in a small area at a certain distance from the advancing crack tip.

In the present study the measurements of SZW, Δa, and X are intended to quantitatively describe these three fracture stages. The procedure adopted for SZW measurements (at mid-thickness) is actually a convenient solution **(11)** with respect to other more sophisticated procedures **(12)** (average values from measurements taken at several positions along the crack front); the values of SZW are intended to account for the amounts of mechanical work spent in plastically deforming the specimens prior to ductile crack extension. On the other hand Δa and X are quantities measured at a critical position along the crack front, to reflect the local nature of cleavage triggering, which is influenced by the stress–strain field and its evolution at the position where cleavage is originated, and possibly by features of the microstructure near to that position. Preliminary analyses via a multiple regression technique performed by one of the authors **(13)(14)** confirmed that optimum correlation between toughness data and fractographic data was provided by the definitions of SZW, Δa, and X adopted here.

A statistical analysis carried out with single and multiple regression methods on the experimental data in Table 2 gave a significant confirmation of good correlations existing among the variables (see Appendix 1 for details). In essence, these analyses led to the conclusion that the variations of the fractographic parameters were statistically significant in accounting for the large variability of J_{inst} data, with all three parameters meaningful in this respect.

The degree of empirical correlation found between the J_{inst} values and the three fractographic parameters indicates that a simple physical link should exist, and a relatively simple equation might provide an interesting picture of the whole failure phenomenon in transition regime. The following equation was chosen to represent the relationship between J_{inst} values and fractographic values

$$J_{inst,\,c} = C_1 \cdot \mathrm{SZW} + C_2 \cdot (\Delta a)^{C_3} + C_4 \cdot X \tag{4}$$

The coefficients C_1, C_2, C_3, and C_4 have been evaluated using a Harwell nonlinear data fitting subroutine, combining features from three different algorithms, namely Newton-Raphson, Steepest Descent, and Marquardt **(15)**. The final solution, in terms of minimum value of a sum of logarithmic errors of *J*-integral, is

$$C_1 = 1.8\ 10^3; \quad C_2 = 2.3\ 10^2; \quad C_3 = 0.70; \quad C_4 = 42$$

(units: *J*-integral in KN/m; SZW, Δa, and X in mm).

The capability of the proposed formula to account for variations in J_{inst} data is shown in Fig. 6. Both the extreme cases, i.e., brittle fractures in the lower shelf region with low toughness values and no stable tearing, and high toughness ruptures near the upper shelf region with extensive plastic yielding

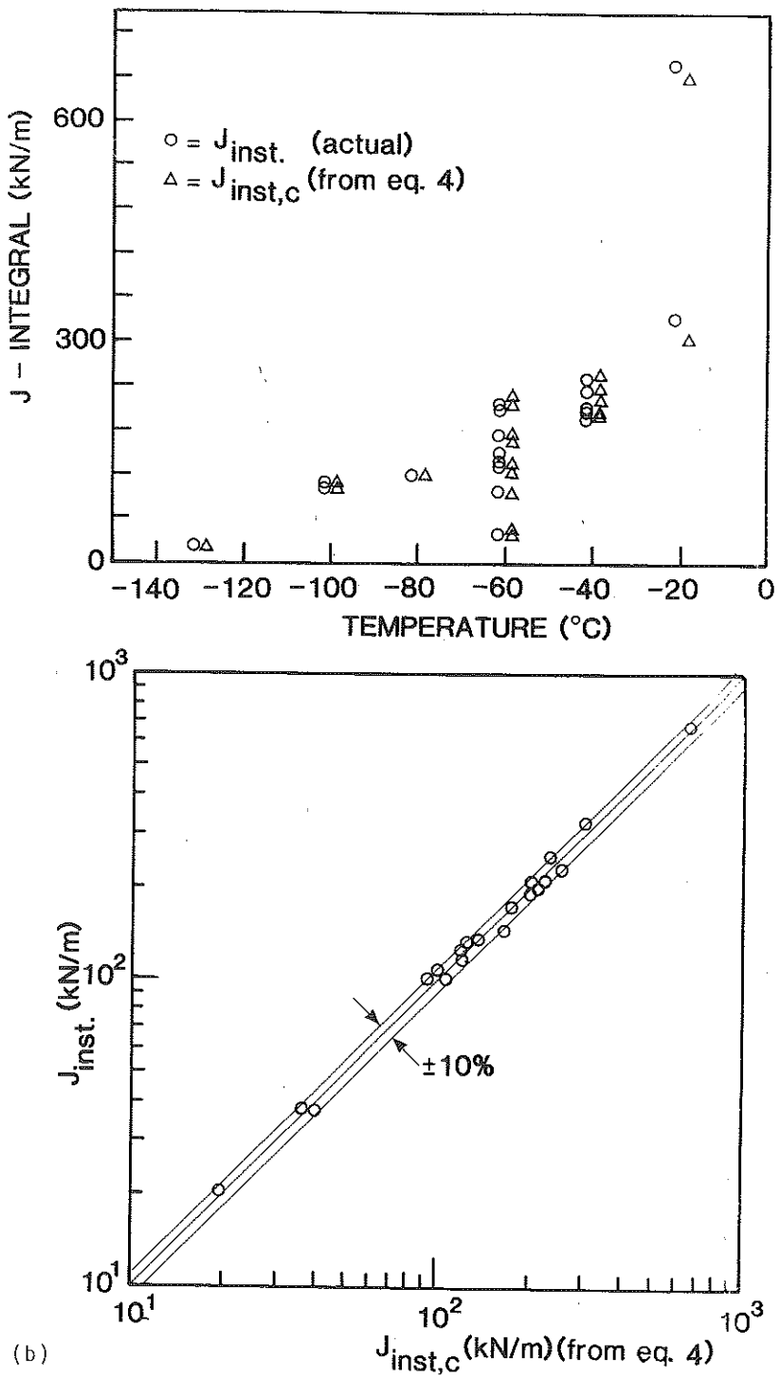

Fig 6 The correlation capability of equation (4): (a) actual values (J_{inst}) and calculated values ($J_{inst,c}$) for the different temperatures of the tests; (b) comparison on logarithmic axes, to appreciate relative errors

and long stable cracks, were successfully accounted, Fig. 6(a). The comparison of actual and calculated values of toughness on the logarithmic scales of Fig. 6(b) allows one to appreciate the relative amounts of the discrepancies, over the wide range of J_{inst} values considered: the average relative error was only 5 percent.

Discussion

According to the J-integral theory, J is a parameter which uniquely characterises the magnitude of stress and strain fields surrounding the tips of stationary cracks; provided certain conditions are met, it still retains this property for an advancing crack too. In addition to this idea of J as a unifying parameter in the functions which describe the stress and strain singularities ahead of cracks, a parallel interpretation of J refers to its energetic definition, as in the original derivation of J by Rice **(16)**. This latter interpretation is still the basis for the formulae used in laboratories to evaluate J from standard EPFM tests: J is essentially measured from areas under load–displacement curves. In the same way in the present study the measurements of J_{inst} represent amounts of mechanical work which were given to the specimens up to the final failures. It comes out that equation (4) bears, therefore, intuitive implications which seem beyond a pure matter of correlating data, and which may be related to the events during which the mechanical work, which is an additive quantity, is progressively fed into the specimen. The global failure energy is viewed in terms of the contributions of three failure events taking place consecutively. Initially crack tip blunting occurs, mostly up to a critical value of SZW; then the J-integral increases due to tearing; finally the specimen breaks in a brittle manner, and the failure energy spent in this event is taken proportional to the extent of the highly stressed area to be broken, represented by X. This is of course a simplified picture: the quantities SZW, Δa, and X are considered independent variables, each associated with distinct contributions to the global failure energy represented by the J-integral; temperature dependence of the coefficients Ci is not considered in equation (4) (temperature influences the amounts of SZW, Δa, and X).

This simplified approach gives the possibility to analyse the three energy contributions to the overall J_{inst} values: $J_{sz} = C_1 \cdot \mathrm{SZW}$, $J_{\Delta a} = C_2 \cdot (\Delta a)^{C_3}$ and $J_x = C_4 \cdot X$. This attempt of 'partitioning' is shown in Fig. 7. Over a large interval of the test temperature the blunting part is the largest one, whereas subcritical crack extension energy becomes important only in the proximity of the upper shelf of the toughness versus temperature curve; cleavage contribution to the J-integral is a small one, according to the common observation that the amount of energy spent in creating two new surfaces in a brittle solid is considerably lower than energies spent in plastically deforming the crack tip and in making the crack to advance by ductile tearing.

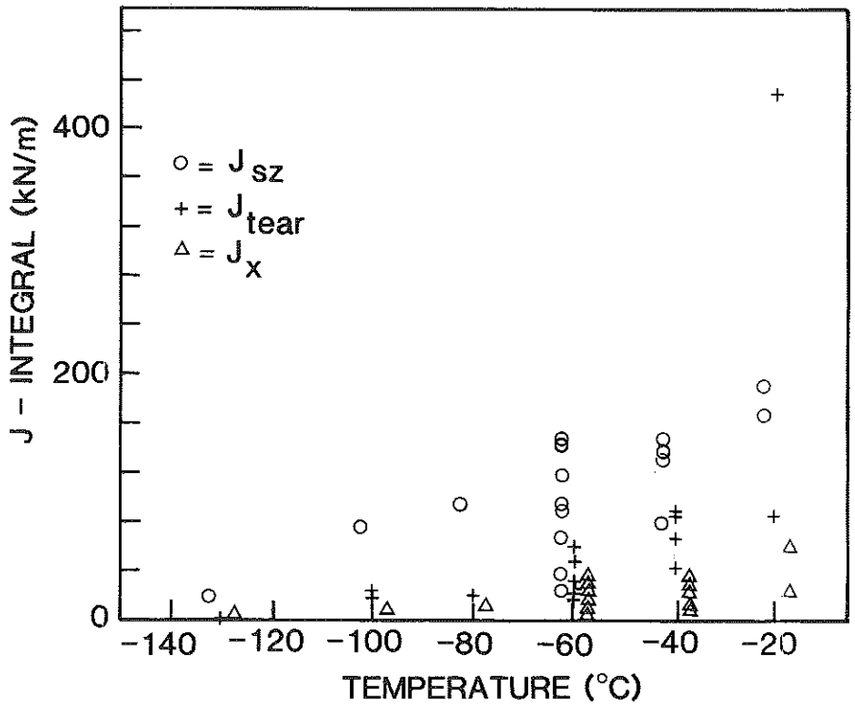

Fig 7 Partitioning the *J*-integral: the different contributions of blunting, tearing, and cleavage

Some similarities with equations usually considered in elastic–plastic fracture mechanics (EPFM) can also be recognised in discussing equation (4). It is seen for example that in the low temperature limit, where $\Delta a \to 0$ and $X \to 0$, the term Jsz is important, and the typical expression of a blunting line is obtained. Interestingly, the value of $1.8 \cdot 10^3$ MPa found here for C_1 is mid-way between the predictions for this steel given by two common models of blunting, ASTM E813–87

$$J = (\sigma_y + \sigma_{uts}) \cdot \Delta a \tag{5}$$

with a blunting line constant of $1.2\ 10^3$ MPa, and Shih–Schwalbe **(17)(18)** model

$$J = \frac{\sigma_0}{0.4\ dn} \cdot \Delta a \tag{6}$$

with a plane strain blunting constant of $2.3\ 10^3$ MPa ($\sigma_y = 0.2$ percent proof stress, σ_{uts} = rupture strength, σ_0 = yield stress, dn = a coefficient defined in Shih–Schwalbe theory; numerical estimates at −80°C). At the high temperature limit where the tearing component in the *J*-integral is important, the typical expression of a *J*–*R* curve is approached by equation (4), in line with standard formulations. The linear dependence on cleavage origin location of the term Jx finally suggests the idea of a constant fracture stress acting over a fracture region of length X. This is similar to the concept of instability occurring when the microscopic cleavage fracture stress σ_f^* is exceeded over a characteristic distance Xo in the Ritchie–Knott–Rice (RKR) model **(19)**. The cleavage origin distance X in the present study is not exactly the same as the 'microstructurally-significant' distance Xo in **(19)**; the X values in Table 2 may however be considered experimental values of the characteristic distance as defined in **(20)(21)** (i.e., the location ahead of the crack tip where the elemental failure probability exhibits a maximum, r_f^*). A trend of increasing values of X with the test temperature is found here, accordingly with the recently recognised temperature dependence of this characteristic distance **(21)(22)**.

It should be noticed that a convenient feature of the present model is the absence of an explicit dependence of the numerical parameters on the test temperature. Temperature is supposed to affect J_{inst} only through variations of SZW, Δa, and X. This seems a reasonable approximation. In the range −130 to −20°C only small variations have to be expected in blunting behaviour (governed by tensile properties), in magnitude of the microstructural fracture stress σ_f^* (for example this quantity is considered temperature-independent in the RKR model; see also the results reported in **(22)**) and in the shape of *J*–*R* curves, which are often found reasonably independent upon test temperature **(1)**. Absence of an explicit temperature dependence allows the derivation of coefficients in equation (4) even from a limited numbers of tests, performed at various temperatures. This is indeed in contrast with the many tests at several defined temperatures typically requested by most statistical approaches to J_{inst} variability analysis. For example the correlation formula proposed by Watanabe *et al.* **(3)** contains temperature dependent coefficients

$$J_{inst,\,c} = A(T) + B(T)(\text{SZW} + \Delta a) + C(T)X \tag{7}$$

This equation seems to give a fit not superior to the present one, even if in **(3)** one hundred fractured specimens were examined, and temperature dependence of the best-fitting coefficients was explicitly allowed. Incidentally, equation (7) does not follow the typical idea of a blunting line from the origin of the J–Δa axes (a quantity $A(T)$ appears in the formula, with uncertain physical meaning), and is also different from current formulations of *J*–*R* curves (power–law relationships are now preferred to linear laws). On the other hand it is noted that in **(3)** a simplified version of equation (7) was demonstrated amenable for analyses through Weibull statistics: cumulative probability diagrams and lower bound curves with definite occurrence probability were obtained. Possibile developments in this direction for the present study are in progress.

Table 4 Results of statistical analysis on data in Table 2

Data set	n	*Type of fit*	*Student's t relative to*			*Multiple correlation coefficient*	*Standard error of the estimate*	*Fisher's*	*Residual variance*
			SZW	Δa	X	R		F	(%)
All 1TCT of Table 2	23	Multiple linear regression	18.0	18.3	2.76*	0.996	13.12	765	0.8
1TCT plate X LT	11	Multiple linear regression	20.9	34.5	3.31*	0.9997	5.36	4018	0.06
All 1TCT of Table 2	23	Equation (4)	19.06	23.26	1.35	0.9974	10.41	1222	0.52
1TCT plate X LT	11	Equation (4)	20.04	34.7	3.206*	0.9997	5.33	4060	0.06
1TCT with $\Delta a < 100$ μm	15	Equation (4)	8.22	4.61	4.46†	0.9983	3.94	1073	0.34

* Significant at 5 percent probability level
† Significant at 0.5 percent probability level

Conclusions

The conclusions of the fractographic investigation performed on 23 1TCT specimens of A533B steel failed by cleavage instability at transition temperatures can be summarised as follows.

(1) The possibility to locate the cleavage origins on the fracture surfaces of specimens of A533B steel broken in the transition region was demonstrated.
(2) An accurate investigation of the nature of the cleavage origins gave poor experimental evidence about the role of carbides in triggering cleavage instability.
(3) Systematic measurements of three fractographic parameters, chosen representative of the different fracture events involved, namely blunting, tearing, and cleavage, gave data well correlated with the J-integral values measured at the instants of instability, J_{inst}.
(4) To rationalise the variability of J_{inst} data, a relationship expressing J_{inst} in terms of distinct contributions from the three fracture events was considered. For the dependence of each contribution on the corresponding fractographic parameter, a simple form was chosen, in analogy with widely accepted EPFM models.
(5) The proposed formula utilizes temperature-independent coefficients and is suitable for application even to small numbers of test data. Actually it was proved capable to account for variations of J_{inst} data within only 5 percent average deviation.

On the basis of these results it seems that simple fractographic measurements might be of help in setting up appropriate toughness data reduction procedures over relatively small sets of tests in the transition region.

It is believed that the basis for studies aimed at developing truly predictive models for failures of SA533B in the transition region should consider in a combined physical and statistical approach the problem of the conditions which trigger the onset of cleavage instability; this problem was not considered in the present work.

Table 3 Values of partial correlation coefficients between the variables considered

	SZW	Δa	X	J_{inst}
SZW	1.000	0.403	0.561	0.763
Δa	0.403	1.000	0.793	0.891
X	0.561	0.793	1.000	0.854
J_{inst}	0.763	0.891	0.854	1.000

Acknowledgements

The authors are strongly indebted to Dr F. Rinaldi (CISE consultant) for discussions and helpful suggestions. Support to this research by ENEL–DSR (Italian Electricity Board–R and D division) under grant ISMAT900 is also gratefully acknowledged.

Appendix

In order to analyse the relationships among the parameters J_{inst}, SZW, Δa, and X, the values of the partial correlation coefficients have been calculated and are reported in Table 3. The most strictly correlated couples of variables are $\Delta a - X$, $J - \Delta a$, and $J - X$, as noticed also by other authors **(1)(3)(9)**.

The first part of the subsequent Table 4 reports results of a multiple linear regression analysis performed on the data of Table 2, and also on a subset of data (11 specimens from plate X in LT orientation). Despite the limited number of observations, very high values are obtained for Student's t associated with the correlation coefficients relative to SZW and Δa. The correlation coefficient relative to X, however, is significant at 5 percent probability level only. The quite large values of the multiple correlation coefficient R and of Fisher's F parameter for the most homogeneous group of data (X plate, LT orientation) are noticeable.

The second part of Table 4 shows the same set of statistical parameters from the VA05A Harwell least square subroutine used to determine the coefficients in equation (4), on the same groups of data and on a subset of 15 specimens having $\Delta a < 100$ μm, from all plates. The situation for SZW and Δa remains almost unaltered, whereas considering the whole sample (three plates and two orientations) the correlation coefficient relative to X is less significant, due to the low contribution of Jx to J_{inst}, with respect to the large contributions of Jsz and $J\,\Delta a$. Actually the Student's t relative to X is significant at 0.5 percent probability level for the group of specimens failed with $\Delta a < 100$ μm. This seems to confirm that the role of X cannot be neglected, particularly when considering groups of specimens failed after small amounts of Δa.

References

(1) DEDOVIC, S., BAKKER, A., and LATZKO, D. G. H. (1988) *Fatigue Fracture Engng Mater. Structures*, **11**, 251–266.
(2) ROSENFIELD, A. R., SHETTY, D. K., and SKIDMORE, A. J. (1983) *Met. Trans*, **14A**, 1934–1937.
(3) WATANABE, J., IWADATE, T., TANAKA, T., YOKOBORI, T., and ANDO, K. (1987) *Engng Fracture Mech.*, **28**, 589–600.
(4) LANDES, J. D. and SHAFFER, D. H. (1980) *Fracture Mechanics: 12th Conference, ASTM STP* **700**, ASTM, Philadelphia, pp. 368–382.
(5) WALLIN, K. (1984) *Engng Fracture Mech.*, **19**, 1085–1093.
(6) SLATCHER, S. (1986) *Fatigue Fracture Engng Mater. Structures*, **9**, 275–289.
(7) NEVILLE, D. J. (1987) *Int. J. Fracture*, **34**, 309–315; (1987) *Engng Fracture Mech.*, **27**, 143–155.

(8) IWADATE, T., TANAKA, Y., TAKEMATA, H., and KABUTOMORI, T. (1985) *Nucl. Engng Des.*, **87**, 89–99.
(9) ROSENFIELD, A. R. and SHETTY, D. H. (1985) *Elastic–plastic fracture test methods: the user's experience, ASTM STP 856*, pp. 196–209, ASTM, Philadelphia.
(10) BARBESINO, F., FOSSATI, C., and RAGAZZONI, S. (1983) *Proc. 5th Int. Conf. on Pressure Vessel Technology*, The American Society of Mechanical Engineers, New York, Vol. **2**.
(11) Recommended standard *JSME S 001–1981*. See also: KOBAYASHI, H., NAKAMURA, H., and NAKAZAWA, H. (1985) *Elastic–plastic fracture test methods: the user's experience, ASTM STP 856*, pp. 3–22, ASTM, Philadelphia.
(12) SCHWALBE, K. H., NEALE, B., and INGHAM, T. (1988) Draft EGF recommendations for determining the fracture resistance of ductile materials: EGF procedure EGF P1–87D, *Fatigue Fracture Engng Mater. Structures*, **2**, 409–420.
(13) RINALDI, F. and RINALDI, C. (1987) CISE Report **3660**.
(14) RINALDI, F. and RINALDI, C. (1988) 16th Plenary Meeting of EGF Task Group I, EPFM, Paris–La Defense (Abstract).
(15) Harwell Subroutine Library (1978) *AERE-R* **9185**, VA05A, Harwell (UK).
(16) RICE, J. R. (1968) *J. Appl. Mech.*, **35**, 379–386.
(17) SHIH, C. F. (1981) *J. Mech. Phys Solids*, **29**, 305–326.
(18) HEERENS, J., SCHWALBE, K. H., and CORNEC, A. (1985) Paper presented at the 18th National Symposium on Fracture Mechanics, Boulder, CO.
(19) RITCHIE, R. O., KNOTT, J. F., and RICE, J. R. (1973) *J. Mech. Phys Solids*, **21**, 395–410.
(20) LIN, T. and RITCHIE, R. O. (1988) *Engng Fracture Mech.*, **29**, 697–793.
(21) LIN, T., EVANS, A. G., and RITCHIE, R. O. (1986) *Acta Met.*, **34**, 641–651.
(22) BOWEN, P., DRUCE, S. G., and KNOTT, J. F. (1987) *Acta Met.*, **35**, 1735–1746.